Neurotoxicology 72 (2019) 51–60

Contents lists available at ScienceDirect

Neurotoxicology

journal homepage: www.elsevier.com/locate/neuro

Full Length Article

Rho-inhibition and neuroprotective effect on rotenone-treated dopaminergic neurons *in vitro*

Letizia Mattii[a,d], Carla Pardini[b], Chiara Ippolito[a], Francesco Bianchi[a], Antonietta Raffaella Maria Sabbatini[c], Francesca Vaglini[b,*]

[a] Department of Clinical and Experimental Medicine, Unit of Histology, via Roma 55, University of Pisa, 56126 Pisa, Italy
[b] Department of Translational Research and of New Surgical and Medical Technologies, via Roma 55, University of Pisa, 56126 Pisa, Italy
[c] Department of Surgical, Medical and Molecular Pathology and Critical Care Medicine, via Roma 55, University of Pisa, 56126 Pisa, Italy
[d] Interdepartmental Research Center Nutraceuticals and Food for Health, University of Pisa, 56124 Pisa, Italy

ARTICLE INFO

Keywords:
Mesencephalic cell culture
Rotenone
RhoA
RhoA inhibitors
α-Synuclein
Connexin 43

ABSTRACT

Mesencephalic cell cultures are a good model to study the vulnerability of dopaminergic neurons and reproduce, *in vitro,* experimental models of Parkinson's disease. Rotenone associated as an environmental neurotoxin related to PD, is able to provoke dopaminergic neuron degeneration by inhibiting complex I of the mitochondrial respiratory chain and by inducing accumulation of α-synuclein. Recently, rotenone has been described to activate RhoA, a GTPase protein.

In the present study we evaluated a possible neuroprotective effect of Rho-inhibitor molecules on rotenone-damaged dopaminergic (DA) neurons obtained from mouse primary mesencephalic cell culture.

Our results showed that Clostridium Botulinum C3 toxin (C3) and simvastatin, as RhoA inhibitors, were able to protect DA neurons from rotenone damages. In fact, pretreatment with C3 or simvastatin significantly prevented the reduction of [^{3}H]dopamine uptake, neurites injury and the expression patterns of proteins like α-syn, actin and connexin 43.

1. Introduction

Pesticides, herbicides and other environmental neurotoxins may be involved in the etiology of several neurodegenerative diseases. Rotenone, a flavonoid widely used as a natural pesticide, is able to induce central nervous system and systemic toxicity (Testa et al., 2005; Cicchetti et al., 2009) by interacting with mitochondria at complex I of the respiratory chain level. Particularly, rotenone is able to induce dopaminergic neuron degeneration and to reproduce, *in vitro* and *in vivo*, experimental models of Parkinson's disease (PD) (Chou et al., 2010; Zhang et al., 2016; Sun et al., 2017). Rotenone major effect is related to dopaminergic (DA) neurons damages which means that it induces reactive oxygen species (ROS) production, inhibits complex I of the mitochondrial respiratory chain and induces the accumulation of α-synuclein (α-syn) in the cytoplasm and neurites.

The direct interactions of this pesticide with tubulin and the inhibition of microtubules assembly have also been described as a possible contribution of its neurotoxic effect (Ren et al., 2005; Ren and Feng, 2007)

Indeed, although the cause of PD remains unclear, it was well documented that the selective death of DA neurons in the substantia nigra pars compacta (SNpc) of the mesencephalon is the main pathological change of this neurodegenerative disorder (Mhyre et al., 2012).

Rho proteins, involved in cell proliferation, cellular migration, polarity and morphogenesis, are GTPases mainly acting on the cytoskeleton (Hall, 2005). In neurons, they can regulate dendritic and axonal outgrowth (Auer et al., 2011). Interestingly, it has been demonstrated that rotenone induces Rho activation in hippocampal or cerebrocortical neurons (Sanchez et al., 2008; Fujimura and Usuki, 2012).

In the present study, we investigated the possible neuroprotective effect of Rho-inhibitor molecules by using an *in vitro* model of PD based on primary mouse mesencephalic cell cultures treated with rotenone (Radad et al., 2006). Accordingly, after verifying rotenone-induced Rho-activation in this experimental scheme, we explored some phenotypic aspects of rotenone-damaged DA neurons and we analyzed them after pre-treatment with Clostridium Botulinum C3 toxin (C3). More specifically, dopamine uptake and neurites growth as well as RhoA, α-syn, tubulin, actin and connexin (Cx) Cx43 expression were investigated. Finally, some of the experiments have been performed also by using simvastatin, a statin that inhibits the rate-limiting enzyme for

* Corresponding author.
E-mail address: francesca.vaglini@med.unipi.it (F. Vaglini).

https://doi.org/10.1016/j.neuro.2019.02.006
Received 7 November 2018; Received in revised form 6 February 2019; Accepted 8 February 2019
Available online 12 February 2019
0161-813X/

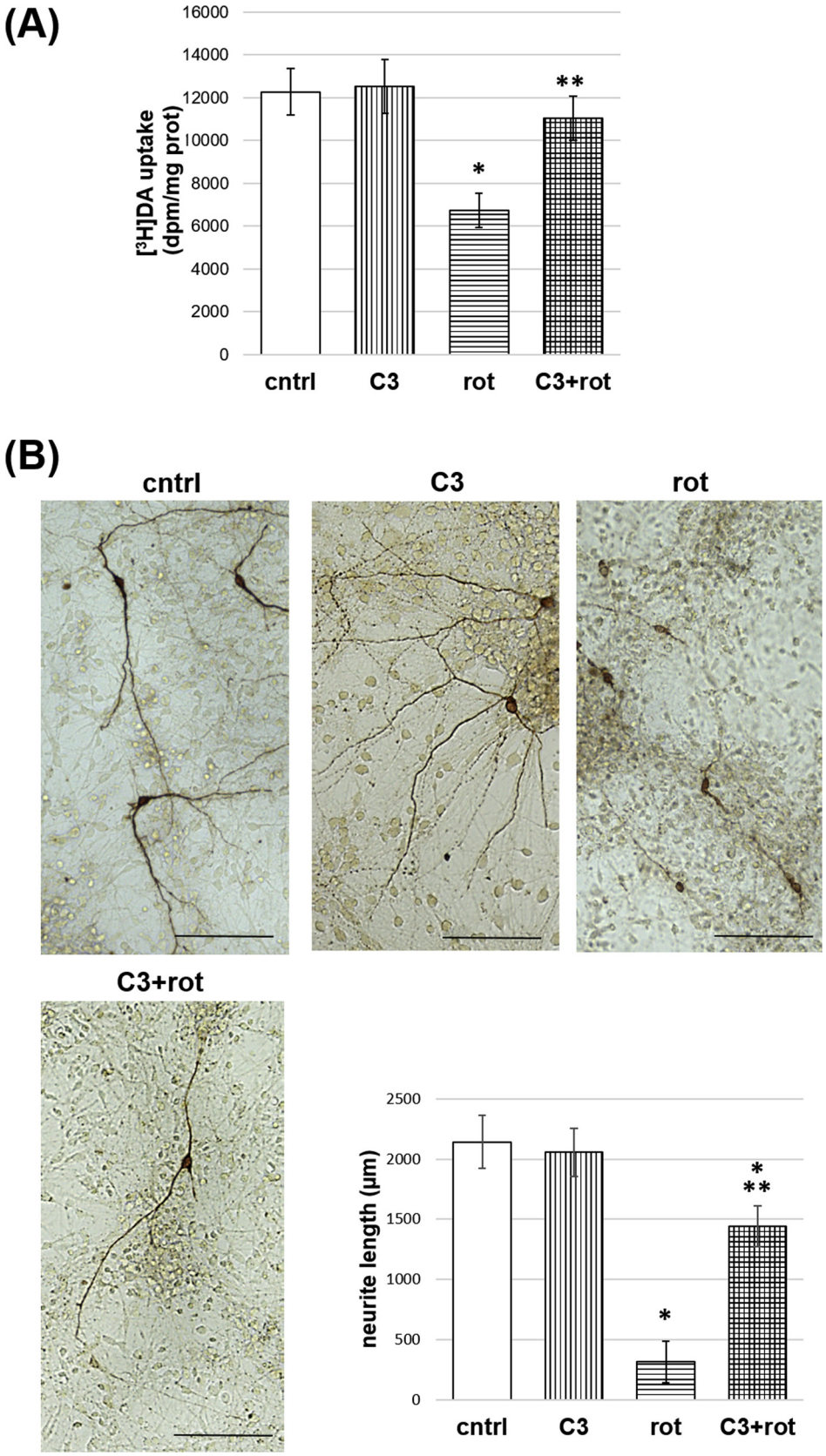

Fig. 1. Effect of C3-treatment on the rotenone-induced DA cell damage. A) After 6 DIV mesencephalic cell cultures were exposed to C3 and four hours later rotenone was added. Twenty-four hours later, [^{3}H]DA uptake was performed. Values represent means ± S.E.M. *$p < 0.01$ vs cntrl; **$p < 0.01$ vs rotenone. B) Representative images of TH immunoperoxidase stained neurons after different treatments. Scale bar: 100 µm.

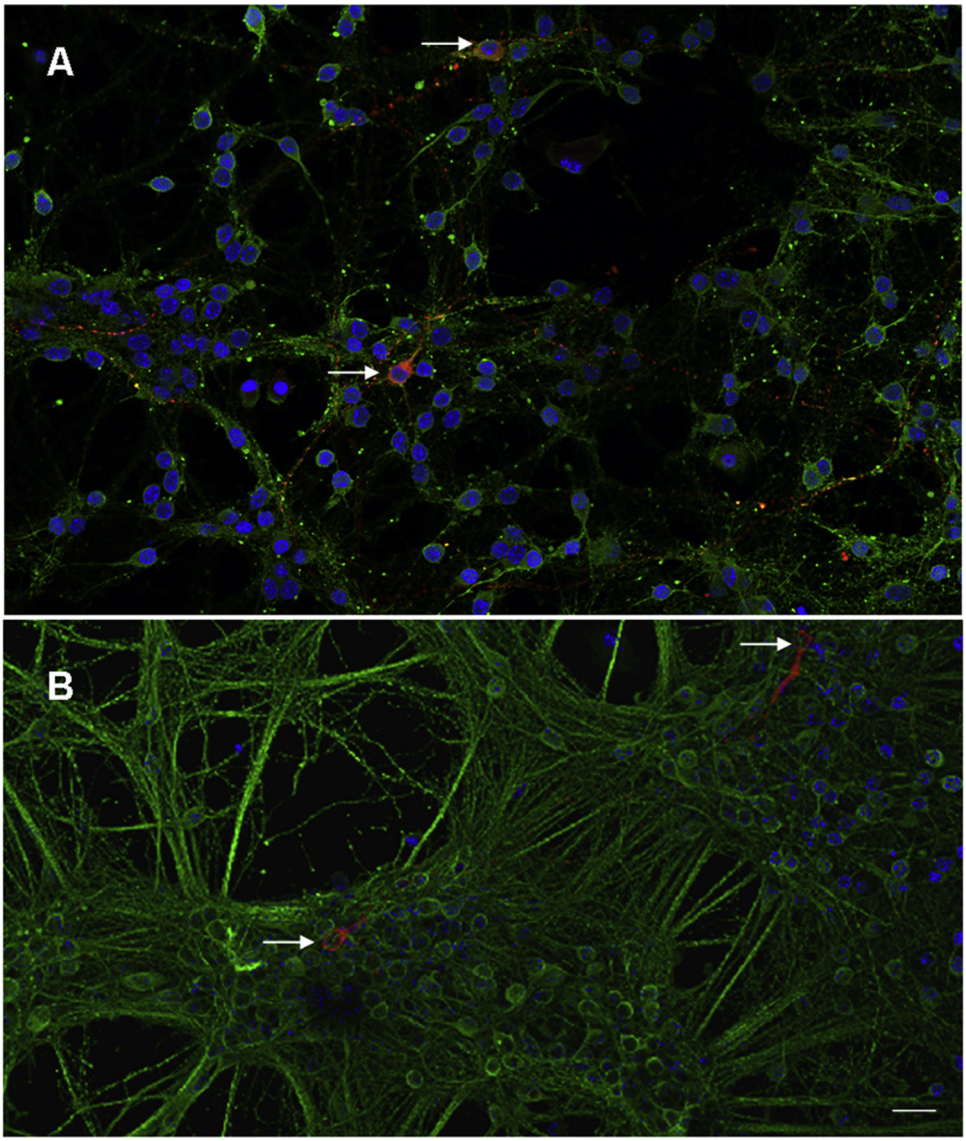

Fig. 2. Immunofluorescent staining of mesencephalic cell cultures containing DA neurons (arrows). Representative images of maximum projection: (A) mesencephalic cells immunostained for TH (red) and RhoA (green) and (B) for TH (red) and α-tubulin (green). Blue colour (TO-PRO staining) marks cell nuclei. Scale bar: 20 μm (For interpretation of the references to colour in this figure legend, the reader is referred to the web version of this article).

cholesterol synthesis. Simvastatin has been suggested to exert a neuroprotective role in neurological diseases such as PD (Bar-On et al., 2008) and it is also another Rho-inhibitor agent.

2. Material and methods

2.1. Chemicals

Eagle's minimum essential medium (MEM), Ham's nutrient mixture F-12, L-glutamine, phosphate buffer saline (PBS) were purchased from Sigma Aldrich (St. Louis, MO, USA). NU-serum V was purchased from Collaborative Research (BD Biosciences, Steroglass, Italy); Cytosine arabinoside was from Upjohn. The Vectastain Elite ABC kit was purchased from Vector Laboratories (Burlingham, CA, USA), CytoScint (ICN Research Products, Costa Mesa, CA, USA). TO-PRO®-3stain was from Life Technologies Italia (Monza, MB, Italia). Phalloidin-iFluor 555 reagent was from Abcam (Cambridge, UK)

All tissue culture supplies were provided by Falcon and Costar.

2.2. Antibodies

Rabbit anti-tyrosine hydroxylase antibody (RαTH) was purchased from Chemicon (ab 152) (Temecula, CA, USA) and Goat anti-α-synuclein antibody (GαSyn) was from Abcam (ab85862). Mouse anti-RhoA antibody (MαRhoA) was from Thermo Scientific (1B3-4A10, Waltham, Massachusetts, USA). Mouse anti-α-Tubulin antibody (MαT) was purchased from Sigma-Aldrich (T5168). Mouse anti-Cx43 antibody (MαCx43) was purchased from Santa Cruz Biotechnology (CXN-6, sc-59949, Santa Cruz, CA, USA). Alexa Fluor® 488 anti-mouse, Alexa Fluor® 568 anti-rabbit and Alexa Fluor® 488 anti-rabbit were purchased from Life Technologies Italia.

2.3. Mouse mesencephalic cell cultures

Timed pregnant CD1 mice were obtained from our laboratory. The animals were handled in accordance with the Guidelines for Animal Care and Use of the National Institutes of Health (NIH Publications No. 8023, revised 1978), and all efforts were made to minimize animal suffering and to keep the number of animals used to a minimum. Brains

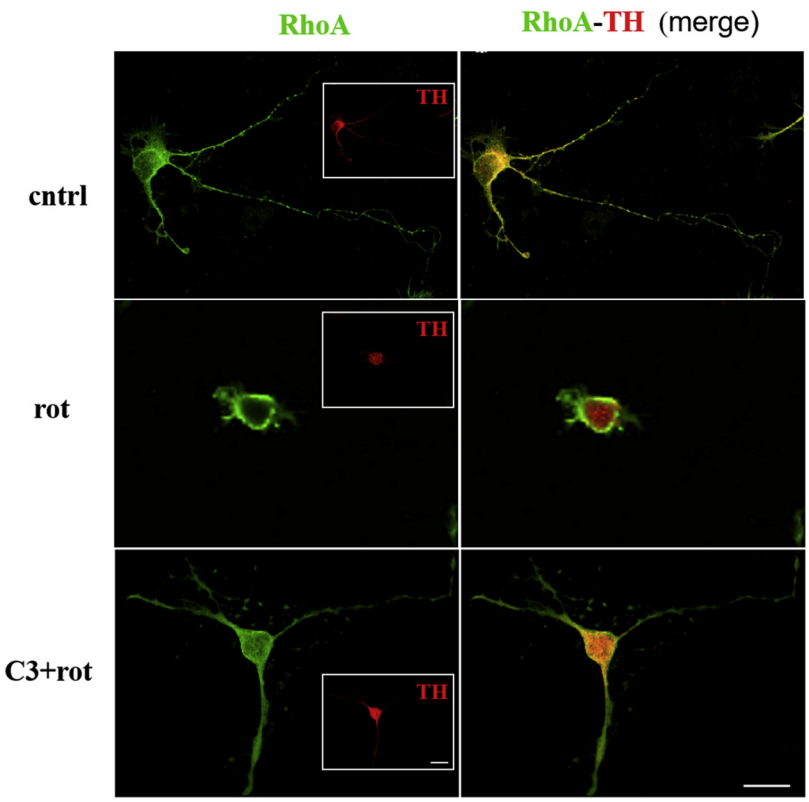

Fig. 3. Effect of rotenone and C3 on RhoA expression. Representative images of DA neurons immunostained for TH (red) and RhoA (green). Cells were treated with rotenone (rot) or C3 + rotenone (C3 + rot); control cells (cntrl) were received only vehicle. Scale bar: 20 μm. (For interpretation of the references to colour in this figure legend, the reader is referred to the web version of this article).

were obtained from 13-day-old mouse embryos and placed in cold, sterile, phosphate-buffered saline (PBS). As previously described (Giorgi et al., 2015), the midbrain was dissected out under microscopic control and placed in a nutrient medium composed of F12 and Eagle's minimal essential medium (ratio1:1), supplemented with 2 mM glutamine, 10% of Nu-serum and 33.3 mM glucose. The tissue was mechanically dispersed, centrifuged at 800 *g* for 3 min, and suspended in the culture medium. Cells were plated at a density of 5×10^5 in 12 multiwell plates or at a density of 1×10^3 in chamber slides (Lab-Tek II Chamber Slide size 8 well). Multiwell plates or chamber slide surfaces were pre-coated with 15 μg/ml of poly-D-lysine (high Mw, > 300,000). The cultures were maintained in a humidified atmosphere of 5% CO2/95% air at 37 °C. Experiments were performed in the absence of glial cells. To obtain virtually pure neuronal cultures, 10 μM cytosine arabinoside (Ara C) which suppresses glia proliferation, was added 3 days after plating (Vaglini et al., 2008).

2.4. Experimental scheme

On day 6 after plating, cells were treated with or without 2.5 μg/ml of C3 and, four hours later, 25 nM of rotenone, was added. Rotenone was prepared in dimethyl sulfoxide (DMSO) (stock solution 1 mM) and diluted with the culture medium. After 24 h, cells were functionally tested for [^{3}H]DA uptake (control cells was 12,277 ± 1096 dpm/mg prot). In addition, a separate set of cells were fixed in paraformaldehyde (4% in PBS) and stored at 4 °C until immunoperoxidase staining and double immunofluorescence analyses were performed.

In another set of experiments, on day 6 the cells were treated with 0.1 μM of simvastatin (stock solution 1 μM dissolved in DMSO) and, four hours later, 25 nM of rotenone was added. After 24 h, [^{3}H] DA uptake was performed (control cells was 15,525 ± 1398 dpm/mg prot). Immunoperoxidase analysis was performed in a separate set of cells that were fixed in paraformaldehyde (4% in PBS). The experiments were performed in triplicate and repeated at least three times.

2.5. Assay of dopamine uptake

[^{3}H]DA uptake was used as a functionality/viability cell characterization. To perform this test, mesencephalic cultures were rinsed with PBS, and incubated for 15 min with 50 nM [^{3}H]DA (23.9 Ci/mmol) at 37 °C. Uptake was stopped by removing the reaction mixture containing the radio-ligand, and rinsing the wells three times with ice-cold PBS. The cells were scraped into 0.5 ml of 0.2 N NaOH containing 0.2% Triton X-100; then 0.5 ml of HCl 0.2 N was added to neutralize the pH. Blank values were obtained by incubating cells at 0 °C, a condition that blocked specific uptake *in vitro*. The radioactivity was counted with 10 ml of Cytoscint (ICN) in a liquid scintillation-counter (Wallac). The results are expressed as percentage of disintegration per minute (dpm), based on three experiments performed in triplicate wells.

2.6. Tyrosine-hydroxylase immunoperoxidase analysis for neurites growth and morphology evaluation

In mesencephalic cultures, fixed in 4% paraformaldehyde for 1 h, DA neurons were identified by using RαTH (Vaglini et al., 2008). In brief, cell cultures were washed twice in PBS, and incubated overnight at 4 °C with the RαTH diluted 1:1000 in PBS containing 0.2% of Triton X-100. Cultures were then washed with PBS, and incubated with a biotinylated anti-rabbit IgG followed by incubation with an avidin-biotin conjugated of peroxidase. The peroxidase was visualized using diaminobenzidine and hydrogen peroxide. To quantify the effect of rotenone on neurites outgrowth in plate, TH + cell were analyzed in ten randomly selected fields (1.13 mm^2/field) at 20x magnifications with a Nikon inverted microscope. Each neuron was outlined manually, and the single axon lengths were evaluated by Axiovision software (The Math Works, Inc., Natick, MA. USA).

2.7. Extraction of unassembled tubulin

The extraction of unassembled tubulin was carried out according to

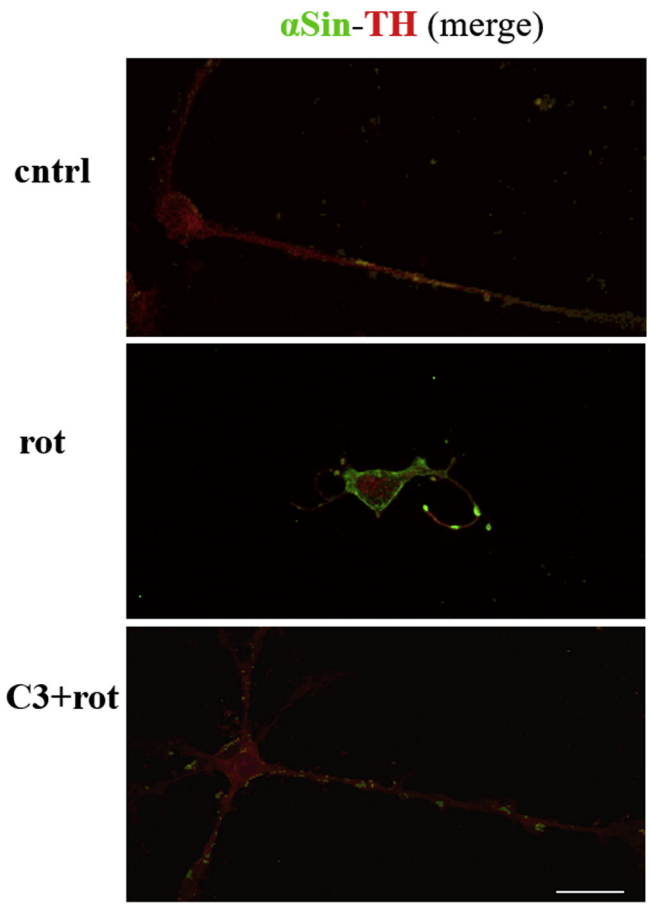

Fig. 4. Effect of rotenone and C3 on α-synuclein expression. Representative images of DA neurons immunostained for TH (red) and α-synuclein (green). Cells were treated with rotenone (rot) or C3 + rotenone (C3 + rot); control cells (cntrl) were received only vehicle. Scale bar: 20 μm. (For interpretation of the references to colour in this figure legend, the reader is referred to the web version of this article).

the procedure described by Brown et al., (Brown et al., 1992). Before tubulin immunostaining, the neurons were permeabilized with non-ionic detergent to extract unassembled tubulin, under conditions that stabilized existing microtubules. Briefly, cells were rinsed once with PBS for 5 min, once with PHEM solution (60 mM Pipes, 25 mM Hepes, 10 mM EGTA, 2 mM $MgCl_2$, pH 6,9) for 5 min, and then were incubated for 5 min with PHEM containing 1% saponin, 10 μM taxol and 0.1% DMSO, to extract unassembled tubulin. All the steps were performed at room temperature. Cells were then fixed in paraformaldehyde (4% in PBS) and stored at 4 °C until immunofluorescence analysis was performed.

2.8. Double-immunofluorescence analysis

Slides with PFA-fixed cultures were treated for 10 min with 0.2% triton-X100/PBS and, after 1 h in blocking solution (BS) (BS: 0.1% Tween, 0.25% BSA in PBS), they were incubated overnight at 4 °C with RαTH (1:1000) together with the following primary antibodies diluted in BS as follows: MαRhoA 1:100, MαCx43 1:1000, MαT 1:2000 and GαSyn 1:200. Slides were then washed three times in BS and incubated for 90 min in the dark with relative fluorescent secondary antibodies diluted 1:250 in BS or with phalloidin-iFluor 555 reagent (1:1000 in 1% BSA). Nuclear staining was performed incubating the slides with 1μM TO-PRO for 15 min in the dark. Samples were mounted with PBS-glycerol solution. All steps were performed at room temperature unless otherwise specified. Negative controls for the specificity of secondary antibodies were performed omitting the primary antibodies. The samples were observed with a confocal laser scanning microscope at 20 × 40x and 63x magnification (TC SSP8 Leica Microsystems, Mannheim, Germany) using a 488-nm, 561-nm and 642-nm excitation wavelength lasers. Due to the clear differences in immunoreactivity between treated or not treated samples, we evaluated the intensity of immunofluorescence by optical observation. In particular, the following semi-quantitative scale of immunoreactivity was adopted: none (-), very low (-+), low (+) and high (++) fluorescence intensity. The evaluation was done by two independent observers on about 10 neurons in random fields per sample in each experiment. The DA cell number that presented a specific fluorescence intensity was expressed in percentage ± S.E.M.

2.9. Statistical analysis

Values from assay of [^{3}H]dopamine uptake are presented as mean values ± S.E.M. ANOVA (Scheffe *F* test) was carried out to identify significant differences in [^{3}H]DA uptake and morphological analysis. The null hypothesis was rejected when p was lower than 0.05.

3. Results

3.1. Effect of C3-treatment on the rotenone-induced dopaminergic cell damage

To examine whether C3 was able to protect against rotenone-induced DA cell damage, [^{3}H]DA uptake and morphology evaluation were performed on rotenone-treated mesencephalic cells pre-treated or not with 2.5 μg/ml C3. The results showed that, when compared to control cells, 25 nM rotenone was able to reduce the [^{3}H]DA uptake of 45% (100 ± 8.9% and 55 ± 6.5%; $p \leq 0.01$), while C3-pre-treatment totally prevented the reduction of [^{3}H]DA uptake rotenone-induced (90 ± 9.2% and 55 ± 11.8%; $p \leq 0.01$). Only a non significant 10% of [^{3}H]DA uptake reduction was evaluated between cells exposed to the double treatment (C3 + rotenone) and control cells (90 ± 8.3% and 100 ± 8.9%; $p \geq 0.05$). C3, 2.5 μg/ml, did not interfere with dopamine [^{3}H]DA uptake compared to control cells that received only vehicle (102 ± 10.1% and 100 ± 8.9%; $p \geq 0.05$) (Fig. 1A).

To evaluate the morphology of DA neurons, they were immunostained by TH-immunoperoxidase 24 h after treatments. Relative to control DA neurons, which showed well developed neurites, rotenone-treated cells exhibited a noticeable and significant reduction of neurite length (100 ± 10.2% vs 15 ± 4.9%; $p \leq 0.01$). When the cultures were pre-treated with C3, the damage, induced by rotenone on the neurite length, was significantly prevented (67 ± 7.8% vs 15 ± 4.9%, respectively; $p \leq 0.01$). However, the neurite length remained significantly reduced when compared to untreated cells (67 ± 7.8% vs 100 ± 10.2%; $p \leq 0.01$). 2.5 μM C3 alone did not interfere with the neurites extension in comparison to control cells (95 ± 9.1% and 100 ± 10.2%; $p \geq 0.05$) (Fig. 1B).

3.2. Effect of C3-treatment on the rotenone-induced changes of protein expression patterns in dopaminergic cells

Double immunofluorescence allowed testing the expression of antigens at DA neurons level. In fact, DA neurons can be identified by RαTH (red cells in Fig. 2) and simultaneously marked for other antigens. In neurons, treated as previously described, expression of RhoA, α-syn, α-tubulin, F-actin and Cx43 were tested. The results, obtained by experiments performed in triplicate, showed that rotenone was able to induce a change in the expression of all the tested molecules and that C3 could interfere with rotenone action except for the α-tubulin expression. Moreover, C3 alone did not influence the expression of these molecules, at least at the concentration used in the experiments conducted in the present study (data not shown).

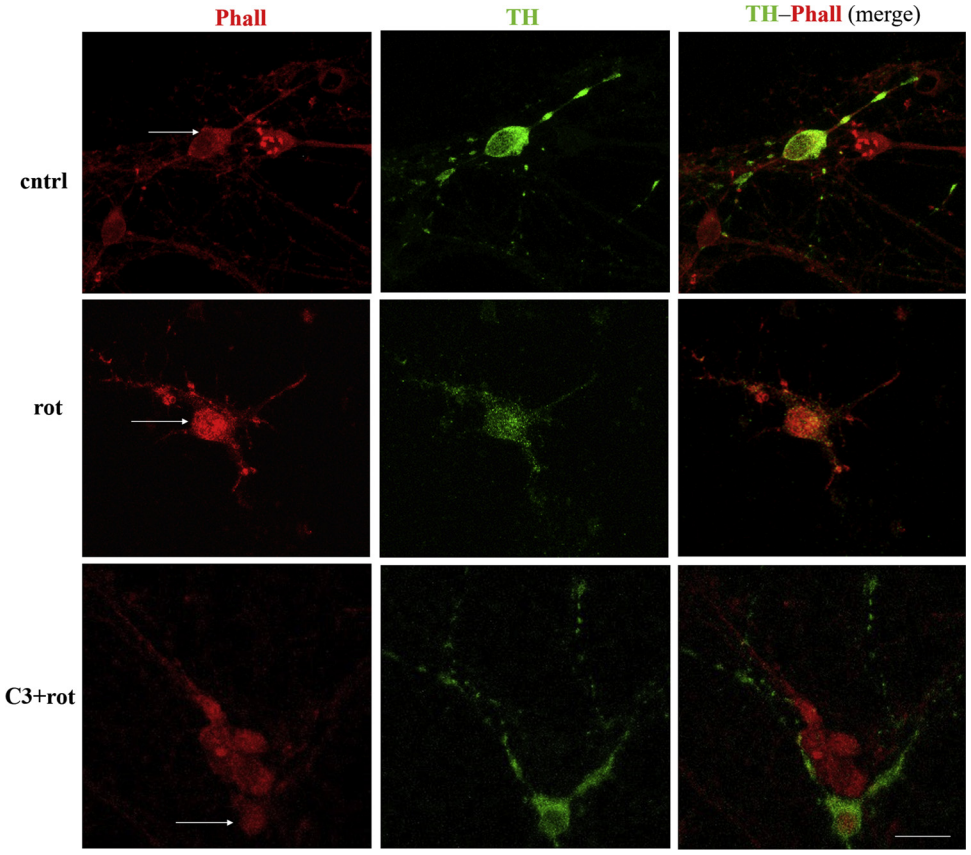

Fig. 5. Effect of rotenone and C3 on F-actin expression. Representative images of DA neurons (arrows) immunostained for TH (green) and F-actin (red) by the use of phalloidin. Cells were treated with rotenone (rot) or C3 + rotenone (C3 + rot); control cells (cntrl) were received only vehicle. Scale bar: 20 µm. (For interpretation of the references to colour in this figure legend, the reader is referred to the web version of this article).

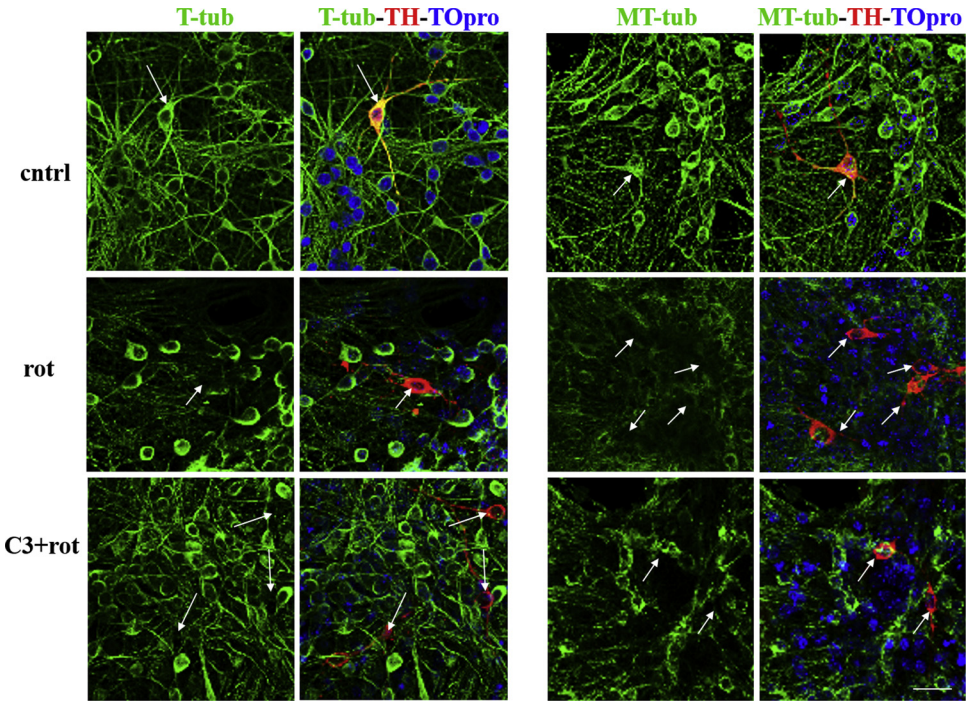

Fig. 6. Effect of rotenone and C3 on tubulin expression. Representative images of DA neurons (arrows) immunostained for TH (red) and total tubulin (T-tub) or microtubular tubulin (MT-tubulin) (green). Cells were treated with rotenone (rot) or C3 + rotenone (C3 + rot); control cells (cntrl) were received only vehicle. Blue colour (TO-PRO staining) marks cell nuclei. Scale bar: 20 µm. (For interpretation of the references to colour in this figure legend, the reader is referred to the web version of this article).

In particular, rotenone induced the activation of RhoA, as it was evidenced by the protein translocation from the cytoplasm to the plasma membrane in DA cells (Fig. 3). Due to this fact, the Rho proteins, indeed, are GTP-bound and located at membrane level when they are activated, while they are GDP-bound and localized at cytoplasm level when they are inactivated (Mattii et al., 2004). The pre-treatment with C3 was able to prevent rotenone-RhoA activation as demonstrated by the RhoA localization at cytoplasm level in DA neurons treated with C3 and rotenone (Fig. 3).

The expression of α-syn was very low (-+) in control cells (94 ± 3%) at level of all cell compartments but it increased (++) in rotenone-treated cells (98 ± 1.8%), mainly at level of the neuronal cell body and varicosities. The expression of α-syn returned to be very low (-+) and similar to control cells, in the combined treated (C3 +

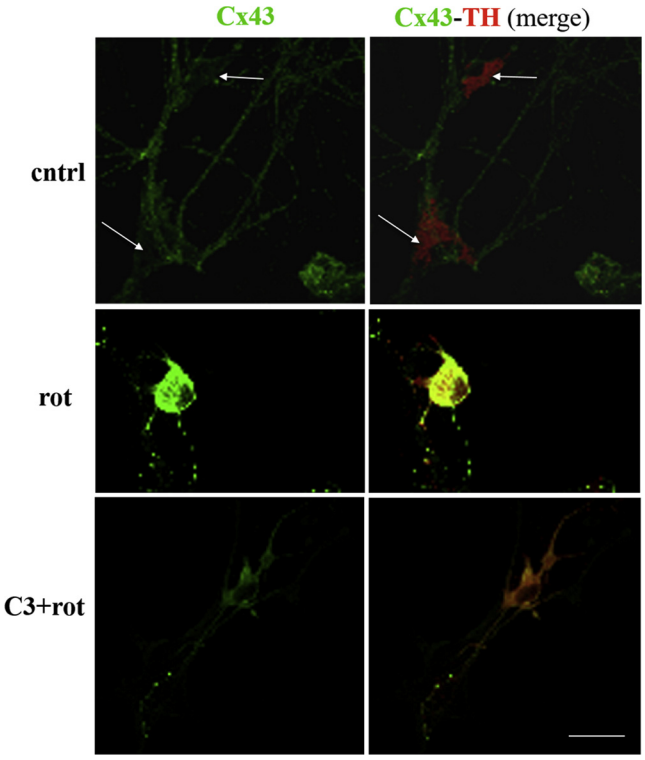

Fig. 7. Effect of rotenone and C3 on Cx43 expression. Representative images of DA neurons (arrows) immunostained for TH (red) and Cx43 (green). Cells were treated with rotenone (rot) or C3 + rotenone (C3 + rot); control cells (cntrl) were received only vehicle. Scale bar: 20 µm. (For interpretation of the references to colour in this figure legend, the reader is referred to the web version of this article).

rotenone) cells (92 ± 2.4%) (Fig. 4).

To assess a possible cytoskeleton alteration, we evaluated actin filaments (F-actin) and α-tubulin expression. Fluorescence of phalloidin, which selectively binds F-actin, appeared very intense (++) in rotenone-treated DA neurons (96 ± 2.1%) compared to control (+, in 100 ± 1.2% cells) and it was evenly distributed in the cytoplasm and neurites, while C3 + rotenone-treated neurons (98 ± 2.1%) resulted less fluorescent (+) and similar to control DA cells (Fig. 5).

Total tubulin (T-tub) as well as assembled tubulin (MT-tub), which represented microtubules, were evaluated. The results showed that DA neurons (100 ± 1.1%) expressed a greater amount of T-tub (++) compared to the assembled one (+/++, in 82 ± 3.2% cells). However, the expression of both T- and MT-tubulin almost disappeared (-+, -) after rotenone treatment in 96 ± 2.2% and 94 ± 2.9 cells, respectively. Interestingly, this rotenone-effect was not reverted by C3-pretreatment either for total or for assembled tubulin. Indeed, the expression of both tubulins was very low (-+, -) in DA neurons treated with C3 plus rotenone (93 ± 2.6% and 96 ± 1.7% cells for T-tub and MT-tub, respectively) and similar to the expression found in rotenone-treated DA neurons (Fig. 6)

Finally, the expression of Cx43, the major astrocytic gap junction protein, which seems to play an important role in PD (Kawasaki et al., 2009), was tested. Cx43 was found in control DA cells with a very faint expression (-+ in 97 ± 1.1% cells) at level of the soma membrane and neurites. In all DA neurons (100 ± 1.1%), rotenone treatment induced an increased expression of Cx43 (++) that was appreciable also at level of the soma cytoplasm and in neurites. C3-pretreatment only partially prevented rotenone-induced Cx43 increase because DA neurons (94% ± 2.3) still showed Cx43 in varicosities and in the soma cytoplasm, albeit in a lesser amount (+) in comparison with rotenone-treated cells (Fig. 7).

3.3. Effect of simvastatin- treatment on the rotenone-induced dopaminergic cell damage

To examine if simvastatin (0.1 µM) was able to protect from rotenone-induced DA cell damage, [^{3}H]DA uptake and morphology evaluation were performed. The results indicated that, when compared to rotenone-induced damage, simvastatin significantly protected DA neurons (51 ± 7.9% vs 74 ± 6.6%; $p \leq 0.01$). However, pretreatment with simvastatin, was unable to restore the [^{3}H]DA uptake value similarly to those of control (74 ± 6.6% vs 100 ± 9.0%; $p \leq 0.01$). Simvastatin alone, did not interfere with the [^{3}H]DA uptake on control cells (108 ± 11% and 100 ± 9.0%; $p \geq 0.05$) (Fig. 8A).

To evaluate the morphology of DA neurons, TH-immunoperoxidase immunostaining was performed 24 h after treatments. Relative to control, TH-positive neurons showed well-developed neurites and rotenone-treated TH-positive neurons exhibited a noticeable and significant reduction of neurite length (100 ± 8.9% vs 15 ± 5.9%; $p \leq 0.01$). Compared to the rotenone treatment, when the cultures were pretreated with simvastatin, the neurite damage was significantly prevented (85 ± 6.8% and 15 ± 5.9%; $p \leq 0.01$), even if the recovery remained significantly different from control (100 ± 8.9% vs 85 ± 6.8%; $p \leq 0.01$).

Moreover, 0.1 µM simvastatin did not interfere with the neurite extension on control cells (98 ± 8.4% and 100 ± 8.9%; $p \geq 0.05$) (Fig. 8B).

4. Discussion

Rotenone, a commonly used plant-derived pesticide, is known to play a role in the pathogenesis of experimental PD (Greenamyre et al., 2010). Sanchez et al. (2008), described that rotenone is able to activate RhoA in neurons. RhoA is a GTPase belonging to the family of Rho proteins and acts as key regulator of several processes associated with changes in the cytoskeleton, such as cell migration, adhesion and contraction (Hall, 2005). RhoA regulates dendritic and axonal outgrowth during development and regeneration mainly through its effect on the cytoskeleton (Auer et al., 2011).

Here, we have reported new insights on molecular effects of rotenone-induced damages on DA neurons and we have shown that C3 and simvastatin could, partially but significantly, prevent them. In our study, we used mesencephalic cell cultures from 13-day-old embryos; after six days *in vitro* they were treated with rotenone at 25 nM, a toxic dose that was able, in our hands, to induce in 24 h, about 50% of functional damage, evaluated as a reduction of [^{3}H]DA uptake. As shown in this paper, rotenone induced cellular pathological changes described also in different PD models (Zeng et al., 2018). In particular, our results demonstrated a significant decrease of both [^{3}H]DA uptake and neurite length in DA neurons after rotenone treatment, compared to control neurons.

Moreover, rotenone-treated cells showed a higher α-syn expression than controls; α-syn expression was characterized with an accumulation in the neurites and with its abnormal distribution. Indeed, Lo Bianco et al. (2002) had described that an overexpression of α-syn in the substantia nigra of rodents with a lentiviral-mediated genetic PD, caused a neurites pathology with distrophic α-syn distribution.

More recently it has been described that an accumulation of α-syn in neuritis was a characteristic of some pathological states, PD included. Neurons showed dystrophic changes characterized by both a neurite retraction and a loss of synaptic connectivity. Indeed, Zhou et al. (2011) demonstrated that in MN9D cells, a DA cell line, the RhoA signalling inhibition by C3 transferase resulted in a neurite extension and was accompanied by a substantial reduction in expression of α-syn mRNA and protein.

Then, we observed in this PD model that rotenone activated RhoA, confirming as described in a different rat PD model (Sanchez et al., 2008). Accordingly, on the base of RhoA literature data (Hall et al.,

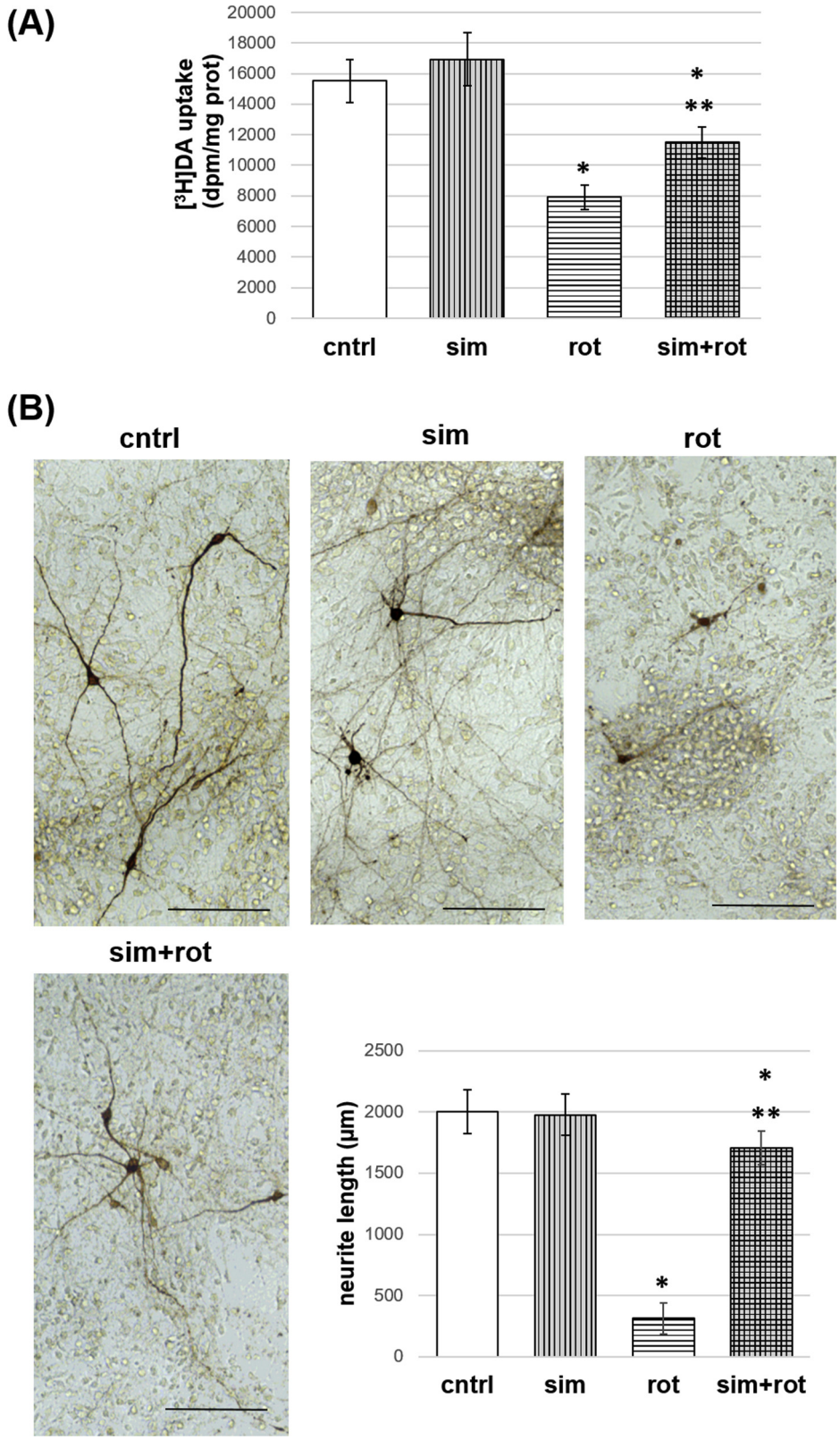

Fig. 8. Effect of simvastatin-treatment on the rotenone-induced DA cell damage. A) After 6 DIV mesencephalic cell cultures were exposed to simvastatin and four hours later rotenone was added. Twenty-four hours later, [^{3}H]DA uptake was performed Values represent means ± S.E.M. *p < 0.01 vs cntrl ; **p < 0.01 vs rotenone B) Representative images of TH immunoperoxidase stained neurons after different treatments. Scale bar: 100 µm.

2005), we expected that rotenone would induce a change in two key components of the cytoskeleton, actin filaments and microtubules. Indeed, after rotenone administration, we found an increased expression of actin filaments and a depolymerisation of microtubules, compared to control cells.

In this PD model, the possible rotenone-induced modulation of Cx43 expression was also explored. Cx43 is a protein belonging to a family of integral membrane proteins that oligomerise to form intercellular

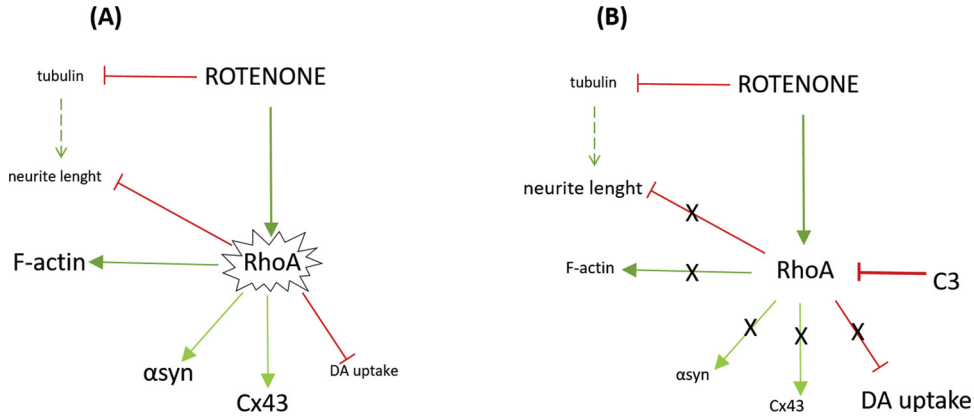

Fig. 9. Summary diagram shows the main findings of this study. A) The effects of RhoA activation induced by rotenone. B) The effects of RhoA inhibition by C3.

channels that arrange gap junctions. These channels are specialized sites of cell-cell contact that allows the passage of molecules with low molecular weight between the cytoplasm of neighbouring cells (Laird, 2006). At central nervous system level (CNS), multiple Cxs are expressed and Cx43 is present both in neurons and in astrocytes, where it is one of the most present (Takeuchi and Suzumura, 2014). In PD animal models, astrocytes showed an upregulation of Cx43 after rotenone treatment (Kawasaki et al., 2009). Regarding our results, DA neurons expressed Cx43 and rotenone was able to upregulate this expression as well. There are still a few studies on the Cx expression and function in neurologic diseases to explain our results. However, recent evidences suggested that the increase in Cx expression, which was observed under pathological conditions, could amplify neuroinflammation and neurodegeneration, probably promoting a shift towards hemichannel activity (Mayorquin et al., 2018). Taken together, the above results about rotenone effects on DA neurons in this PD model are in line with previous studies. Indeed, as described above, rotenone influenced process extension by altering cytoskeleton components, and induced RhoA activation and α-syn increased expression. On the contrary, rotenone involvement on the increased expression of Cx43 in DA neurons, was described, for the first time, in this study. So far few studies about PD model and Cx43 have been carried out regarding only astrocytes (Rufer et al., 1996; Kawasaki et al., 2009; Wang et al., 2013). Certainly, further studies need to be performed to deepen the role of neuronal Cx43 in PD disease.

Fujimura and Usuki (2012) demonstrated that treatment with Rho family inhibitors was able to prevent neuritic degeneration induced by different toxicants including rotenone. Based on these assumptions, as well as on our results about rotenone-induced RhoA activation, we used C3 as an inhibitor of RhoA in this rotenone toxicity model. C3 toxin is an ADP-ribosyltransferase that renders the GTPase proteins biologically inactive (Aktories et al., 1992). In our experiments, we evaluated the effect of C3 pretreatment on rotenone-treated neurons. We used C3 at 2.5 μM concentration that was reported to inhibit RhoA activity in blood cells (Mattii et al., 2004). Our results confirmed that this concentration of C3 inactivated RhoA also in DA neurons, without affecting their viability (data not shown). Moreover, the results demonstrated that C3 pre-treatment offered protection against rotenone toxicity in these neurons through inhibiting RhoA activation. Indeed, suppression of RhoA activity by C3 was related to a decrease or the lack of the rotenone effects observed in this model. However, this was not the case of microtubules disorganization induced by rotenone. An alternative signal pathway, that does not include RhoA, may explain this result but more likely, a direct interaction of rotenone with tubulin and an ensuing microtubule disintegration could be the mechanism involved. Indeed, a recent study (Bisbal et al., 2018) suggests that rotenone-induced microtubule destabilization promotes the expression of Lfc, a guanine nucleotide exchange factor for Rho, with subsequent RhoA activation. Moreover, this mechanism might explain why C3 did not completely reverse the reduction of rotenone-induced neurite length in our experiments (Fig.9). Simvastatin, another Rho inhibiting agent, showed similar behaviour of C3 on DA uptake and neurite length decrease, both induced by rotenone. It is interesting to note that C3 and simvastatin pretreatments gave similar results, although they inhibited RhoA in different manners. In particular, C3 rendered RhoA inactive by ribosylating its effector binding domain while simvastatin inhibited RhoA prenylation and its subsequently trafficking to membranes, a necessity for its normal biological activity. This fact strengthens the notion that pharmacological modulation of Rho GTPase signalling is able to protect cellular and neurite function of damaged DA mesencephalic neurons in this *in vitro* PD model and, at the same time, it also represents an additional confirmation for the similar results obtained in different PD models. On the other hand, a very recent review (Koch et al., 2018) suggests Rho kinase (ROCK), one of the major downstream kinases activated by Rho-GTPase, as a promising drug target for further research in neurodegenerative pathologies.

In conclusion, our results demonstrate that pharmacological modulation of Rho GTPase signalling is able to protect cellular and neurite function of lesioned DA mesencephalic neurons in an *in vitro* model of rotenone-induced PD and they support the statement that C3/statine-like molecules could be potential therapeutic agents for the PD treatment.

Conflict of interest statement

There is no potential conflict of interest or competing interest.

Funding

This work was funded by PRA “Progetti di Ricerca di Ateneo” from the University of Pisa.

Acknowledgements

The authors would like to thank Mr. Sauro Dini, for skillful technical support and Mrs Petra Hrouzkova for English language proofreading.

References

Aktories, K., Mohr, C., Koch, G., 1992. Clostridium botulinum C3 ADP-ribosyltransferase. Curr. Top. Microbiol. Immunol. 175, 115–131.
Auer, M., Hausott, B., Klimaschewski, L., 2011. Rho GTPases as regulators of morphological neuroplasticity. Ann. Anat. 193 (4), 259–266.
Bar-On, P., Crews, L., Koob, A.O., Mizuno, H., Adame, A., Spencer, B., Masliah, E., 2008. Statins reduce neuronal alpha-synuclein aggregation in in vitro models of Parkinson's disease. J. Neurochem. 105 (5), 1656–1667.
Bisbal, M., Remedi, M., Quassollo, G., Cáceres, A., Sanchez, M., 2018. Rotenone inhibits axonogenesis via an Lfc/RhoA/ROCK pathway in cultured hippocampal neurons. J.

Neurochem. 146 (5), 570–584.
Brown, A., Slaughter, T., Black, M., 1992. Newly assembled microtubules are concentrated in the proximal and distal regions of growing axons. J. Cell Biol. 119 (4), 867–882.
Chou, A.P., Li, S., Fitzmaurice, A.G., Bronstein, J.M., 2010. Mechanisms of rotenone-induced proteasome inhibition. Neurotoxicology 31 (4), 367–372.
Cicchetti, F., Drouin-Ouellet, J., Gross, R.E., 2009. Environmental toxins and Parkinson's disease: what have we learned from pesticide-induced animal models? Trends Pharmacol Sci. 30 (9), 475–483.
Fujimura, M., Usuki, F., 2012. Differing effects of toxicants (methylmercury, inorganic mercury, lead, amyloid β, and rotenone) on cultured rat cerebrocortical neurons: differential expression of rho proteins associated with neurotoxicity. Toxicol. Sci. 126 (2), 506–514.
Giorgi, C., Fausto, C., Pardini, C., Simili, M., Del Carratore, R., Vaglini, F., 2015. Effect of itraconazole on mouse mesencephalic neurons. Int. J. Dev. Neurosci. 44, 75–83.
Greenamyre, J.T., Cannon, J.R., Drolet, R., Mastroberardino, P.G., 2010. Lessons from the rotenone model of Parkinson's disease. Trends Pharmacol. Sci. 31 (4), 141–142.
Hall, A., 2005. Rho GTPases and the control of cell behaviour. Biochem. Soc. Trans. 33, 891–895.
Kawasaki, A., Hayashi, T., Nakachi, K., Trosko, J.E., Sugihara, K., Kotake, Y., Ohta, S., 2009. Modulation of connexin 43 in rotenone-induced model of Parkinson's disease. Neuroscience 160 (1), 61–68.
Koch, J.C., Tatenhorst, L., Roser, A.E., Saal, K.A., Tönges, L., Lingor, P., 2018. ROCK inhibition in models of neurodegeneration and its potential for clinical translation. Pharmacol. Ther. 189, 1–21.
Laird, D.W., 2006. Life cycle of connexins in health and disease. Biochem. J. 394, 527–543.
Lo Bianco, C., Ridet, J.L., Schneider, B.L., Deglon, N., Aebischer, P., 2002. α-Synucleinopathy and selective dopaminergic neuron loss in a rat lentiviral-based model of Parkinson's disease. Proc. Natl. Acad. Sci. U. S. A. 99 (16), 10813–10818.
Mattii, L., Fazzi, R., Moscato, S., Segnani, C., Pacini, S., Galimberti, S., D'Alessandro, D., Bernardini, N., Petrini, M., 2004. Carboxy-terminal fragment of osteogenic growth peptide regulates myeloid differentiation through RhoA. J. Cell. Biochem. 93 (6), 1231–1241.
Mayorquin, L.C., Rodriguez, A.V., Sutachan, J.J., Albarracín, S.L., 2018. Connexin-mediated functional and metabolic coupling between astrocytes and neurons. Front. Mol. Neurosci. 11, 118.
Mhyre, T.R., Boyd, J.T., Hamill, R.W., Maguire-Zeiss, K.A., 2012. Parkinson's disease. Biochemistry 65, 389–455.
Radad, K., Rausch, W.D., Gille, G., 2006. Rotenone induces cell death in primary dopaminergic culture by increasing ROS production and inhibiting mitochondrial respiration. Neurochem. Int. 49 (4), 379–386.
Ren, Y., Feng, J., 2007. Rotenone selectively kills serotonergic neurons through a microtubule-dependent mechanism. J. Neurochem. 103, 303–311.
Ren, Y., Liu, W., Jiang, H., Jiang, Q., Feng, J., 2005. Selective vulnerability of dopaminergic neurons to microtubule depolymerization. J. Biol. Chem. 280, 34105–34112.
Rufer, M., Wirth, S.B., Hofer, A., Dermietzel, R., Pastor, A., Kettenmann, H., Unsicker, K., 1996. Regulation of connexin-43, GFAP, and FGF-2 is not accompanied by changes in astroglial coupling in MPTP-lesioned, FGF-2-treated parkinsonian mice. J. Neurosci. Res. 46 (5), 606–617.
Sanchez, M., Gastaldi, L., Remedi, M., Cáceres, A., Landa, C., 2008. Rotenone-induced toxicity is mediated by Rho-GTPases in hippocampal neurons. Toxicol. Sci. 104 (2), 352–361.
Sun, H., He, X., Liu, C., Li, L., Zhou, R., Jin, T., Yue, S., Feng, D., Gong, J., Sun, J., Ji, J., Xiang, L., 2017. Effect of Oleracein E, a neuroprotective tetrahydroisoquinoline, on Rotenone-induced Parkinson's Disease cell and animal models. Chem. Neurosci. 8 (1), 155–164.
Takeuchi, H., Suzumura, A., 2014. Gap junctions and hemichannels composed of connexins: potential therapeutic targets for neurodegenerative diseases. Front. Cell. Neurosci. 8, 189.
Testa, C.M., Sherer, T.B., Greenamyre, J.T., 2005. Rotenone induces oxidative stress and dopaminergic neuron damage in organotypic substantia nigra cultures. Brain Res. Mol. Brain Res. 134 (1), 109–118.
Vaglini, F., Pardini, C., Viaggi, C., Caramelli, A., Corsini, G.U., 2008. Apomorphine offers new insight into dopaminergic neuron vulnerability in mesencephalic cultures. Neuropharmacology 55 (5), 737–742.
Wang, Y., Wu, Z., Liu, X., Fu, Q., 2013. Gastrodin ameliorates Parkinson's disease by downregulating connexin 43. Mol. Med. Rep. 8 (2), 585–590.
Zeng, X.S., Geng, W.S., Jia, J.J., 2018. Neurotoxin-induced animal models of parkinson disease: pathogenic mechanism and assessment. ASN Neuro 10, 1–15.
Zhang, J.Y., Deng, Y.N., Zhang, M., Su, H., Qu, Q.M., 2016. SIRT3 acts as a neuro- protective agent in rotenone-induced Parkinson cell model. Neurochem. Res. 41 (7), 1761–1773.
Zhou, Z., Kim, J., Insolera, R., Peng, X., Fink, D.J., Mata, M., 2011. Rho GTPase regulation of α-synuclein and VMAT2: implications for pathogenesis of Parkinson's disease. Mol. Cell. Neurosci. 48 (1), 29–37.